

V

VOLCANO-ELECTROMAGNETIC EFFECTS

Volcano-electromagnetic effects—electromagnetic (EM) signals generated by volcanic activity—derive from a variety of physical processes. These include piezomagnetic effects, electrokinetic effects, fluid vaporization, thermal demagnetization/remagnetization, resistivity changes, thermochemical effects, magnetohydrodynamic effects, and blast-excited traveling ionospheric disturbances (TIDs). Identification of different physical processes and their interdependence is often possible with multiparameter monitoring, now common on volcanoes, since many of these processes occur with different timescales and some are simultaneously identified in other geophysical data (deformation, seismic, gas, ionospheric disturbances, etc.). EM monitoring plays an important part in understanding these processes.

Brief history

The identification of electromagnetic field disturbances associated with volcanic activity has a relatively young history. Initial measurements in the 1950s on Mihara volcano in Japan focused on monitoring the inclination and declination of the magnetic field while on Kilauea in Hawaii static electric fields (self-potential, SP) were shown to reflect the intrusion activity. More robust magnetic and electric field observations since the 1960s show changes of several tens of nanotesla and more than a hundred mV km^{-1} accompany eruptions from volcanoes (Johnston, 1997; Zlotnicki, 1995). Following eruptions, much larger changes result from remagnetization processes.

Physical mechanisms involved

Short-term magnetic and electric field changes during volcanic eruptions result primarily from stress changes in volcanic rocks and injection of hydrothermal/magmatic fluids and gasses. Of particular importance for research in eruption prediction are changes generated in the early stages of eruptions by deformation and/or fluid/gas flow. Detection of these fields provides an independent window into the eruption process.

The dominant physical processes in play during the final stages before eruptions are stress-induced modification of magnetization (piezomagnetism), electric currents produced by fluid flow (electrokinetic effects), and thermal demagnetization and remagnetization of volcanic rocks. Other EM signals result from charge generation during fluid vaporization and the creation of ash. Changes in EM response also result from modification of the electrical conductivity structure. During and following eruptions, dramatic EM signals can result from electric charge generation from rock disintegration, lightning within the eruption ash cloud, magnetohydrodynamic effects, thermal remagnetization, stress driven magnetization changes, and coupled TIDs.

It has become increasingly clear, because of the complexity and interdependence of volcanic processes, that simultaneous multiparameter monitoring (e.g., strain, fluid pressure, tilt, ground displacement,

electric fields, magnetic fields, gas emissions, etc.) on volcanoes is necessary to identify and separate contributions from the different physical processes. Interpretation of electric and magnetic fields can thus be best done within the constraints placed by other geophysical data and vice versa.

Piezomagnetic effects

The magnetic properties of rocks have been shown under laboratory conditions to depend on the state of applied stress, and theoretical models for this phenomenon have been developed in terms of single domain, pseudosingle domain rotation and multidomain wall translation. The stress sensitivity of magnetization K , defined as the change in magnetization per unit magnetization per unit stress, can be expressed in the form

$$\Delta \mathbf{I} \approx K \sigma \cdot \mathbf{I}, \quad (\text{Eq. 1})$$

where $\Delta \mathbf{I}$ is the change in magnetization in a body with net magnetization \mathbf{I} due to a deviatoric stress σ , K the stress sensitivity, typically has values of about $3 \times 10^{-3} \text{ MPa}^{-1}$. The stress sensitivity of induced and remanent magnetization from theoretical and experimental studies has been combined with stress estimates from dislocation models of fault rupture and elastic pressure loading in active volcanoes to calculate magnetic field changes expected to accompany volcanic activity. These volcanomagnetic models show that moderate scale magnetic anomalies of several nanoteslas (nT) should accompany moderate to large volcanic eruptions for rock magnetizations and stress sensitivities of $1 \text{ Amperemeter}^{-1} (\text{A m}^{-1})$ and 10^{-3} MPa^{-1} , respectively (Johnston, 1997).

Electrokinetic effects

Electrokinetic electric and magnetic fields result from fluid flow through layered volcanic rocks as ions anchored to solid material induce equivalent ionic charge of opposite sign in the fluids. The fluid flow itself is thermally and gravitationally driven. Fluid flow in this system transports the ions in the fluid in the direction of flow, producing electric potential of several tens of mV km^{-1} and magnetic fields of a few nanoteslas.

The current density \mathbf{j} and fluid flow rate \mathbf{v} in porous media are found from the coupled equations

$$\mathbf{j} = -s \nabla E - \frac{\xi \zeta \nabla P}{\eta}, \quad (\text{Eq. 2})$$

$$\mathbf{v} = \frac{\phi \xi \zeta \nabla E}{\eta} - \frac{\kappa \nabla P}{\eta}, \quad (\text{Eq. 3})$$

where E is streaming potential, s is the electrical conductivity of the fluid, ξ is the dielectric constant of water, η is fluid viscosity, ζ is

the zeta potential, ϕ is the porosity, κ is the hydraulic permeability, and P is pore pressure. Unfortunately, many of these parameters are poorly known within volcanoes.

Electrokinetic models combined with estimates of electrical conductivity structure within volcanoes have been proposed to explain the curious “W” form of electric potential commonly observed on active volcanoes (Ishido, 2004).

Electrical resistivity

Changes in electrical resistivity of volcanic rocks result from changes in strain, temperature, chemistry, and fluid content. While little theoretical research has been done on the details of resistivity changes within volcanoes and methods to separate the different contributions, there is no question that resistivity changes occur and are observed during eruptions (e.g., Yukutake *et al.*, 1990; Zlotnicki *et al.*, 2003). Measurement methods include magnetotellurics (MT) and Schlumberger, Wenner, DC/DC, and dipole/dipole systems.

Thermal remagnetization and demagnetization

Rocks lose their magnetization when temperatures exceed the Curie Point ($\approx 580^\circ\text{C}$ for magnetite) and become remagnetized again as the temperature drops below this value. At shallow depths in volcanic regions, particularly in recently emplaced extrusions and intrusions, cracking from thermal expansion allows gas and fluid movement to rapidly transport heat. Large local anomalies of hundreds of nanoteslas from remagnetization of the upper few tens of meters can be generated quickly (Dzurisin *et al.*, 1990). At greater depth these effects occur on very long timescales because of the small thermal conductivity of crustal rocks.

Observations

Volcanomagnetic effects

Unambiguous observations of magnetic field changes have been obtained on many active volcanoes. The best examples clearly related to volcanic activity were obtained during (1) the 18 May 1980, eruption from Mount St. Helens, (2) the 1987 eruption sequence from Piton de la Fournaise, Reunion Island, (3) the 16–22 November 1986, eruption of Izu-Oshima volcano, Japan, (4) the 1980–1990 intrusion episode in Long Valley caldera, California, (5) the 2000 eruption of Miyake-Jima, and (6) the 2003 eruption of Mt. Etna, Italy. Figure V9 shows an example of data from Mount St. Helens during the first stage of the eruption on 18 May 1980. A final magnetic field offset of 9 ± 2 nT was permanent and consistent with pressure decrease within the mountain at the time of the eruption. The net positive signal contrasts with the negative change expected from the removal of magnetic material from the mountain (Johnston, 1997). The oscillatory signals are magneto-gas dynamic effects that couple into the ionosphere and propagate many thousands of kilometers round the world. Figure V10 shows this signal propagating across a 20-station magnetometer array between

1000 and 1500 km from the volcano. These TIDs are commonly generated by explosive volcanic eruptions and earthquakes.

Volcanoelectric effects

A number of important new electric field experiments have focused on obtaining measurements on, or near, active volcanoes. In particular, impressive self-potential observations have been made that delineate the changing electric potentials around erupting volcanoes. SP anomalies show apparent correlation with episodes of intrusive activity, active venting, and eruptions. The pertinent physical mechanisms in this case are electrokinetic effects, fluid vaporization and thermoelectric effects. These are all generated by the injection of hot magma, gas, and hydrothermal fluids into the volcano.

The best documented examples are recorded on:

1. Unzen, Japan, during 1990–1992 where large positive self-potential anomalies were identified in the vicinity of the new lava dome. Potentials generated by fluid flow in the hydrothermal system beneath the array is suggested as the most likely cause for this anomaly.
2. Piton de la Fournaise volcano on Reunion Island, where similar positive self-potential anomalies have been observed above the active magma chamber.
3. Oshima Eruption, Japan, in 1986, where continuous measurements of vertical electric fields in the frequency range 0–3 KHz before,

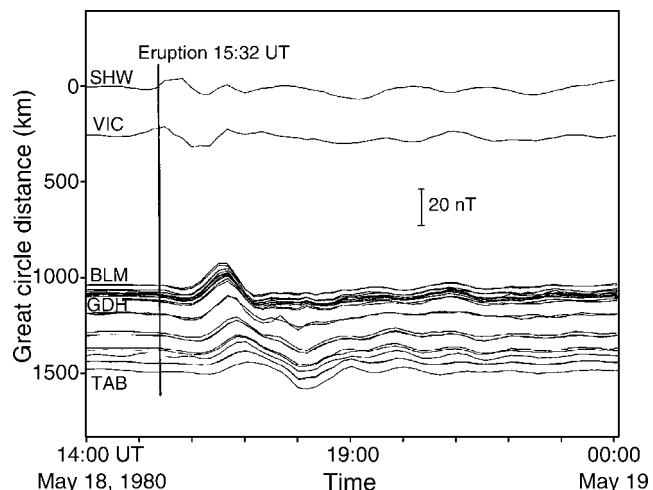


Figure V10 Magnetic field as a function of time and great circle distance following the 18 May 1980 eruption of Mount St. Helens (from Mueller and Johnston, 1989).

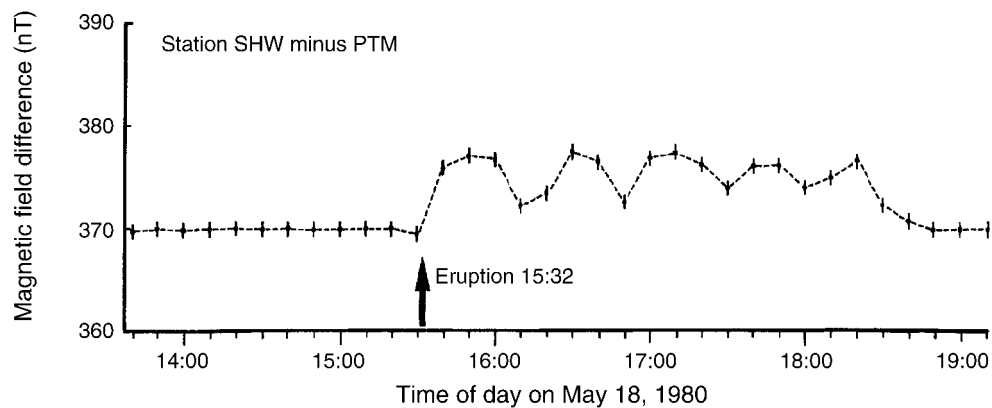


Figure V9 Total magnetic field differences between stations SHW, on Mount St. Helens, and remote reference station, PTM, at Portland Oregon, for the several hours preceding and following the 18 May 1980 catastrophic eruption. Time in UTC (from Johnston *et al.*, 1981).

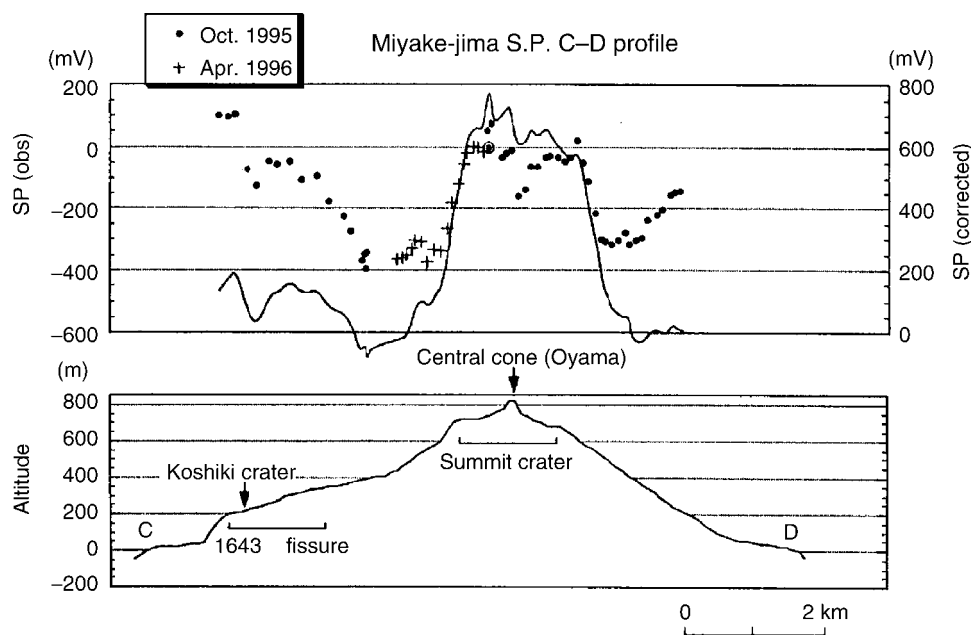


Figure V11 Self-potential profile across Miyake-Jima volcano Japan (from Sasai *et al.*, 1997). The solid line in the upper plot shows the data corrected for elevation effects.

during and after a minor eruption from Mt. Mihara show a series of rapidly rising slow-decaying pulses. These effects are attributed to electrokinetic phenomena in the hydrothermal system.

- Miyake-Jima, Japan, in 2000, where resistivity on scales of 0.5–1.5 km show up to a 300% change before eruptions. Immediately before the onset of caldera formation on 8 July 2000, self-potential near the summit reversed sign from positive to as much as -225mV . Figure V11 shows the SP record from Miyake-Jima about 3 years before the eruption from Sasai *et al.* (1997). Zlotnicki *et al.* (2003) suggest the preeruption observations resulted from electrokinetic effects in a changing hydrothermal system. Re-measurements in 2003 indicate the SP anomalies are much reduced in amplitude and are localized to the edges of the new crater.

M.J.S. Johnston

Bibliography

- Dzurisin, D., Denlinger, R.P., and Rosenbaum, J.G., 1990. Cooling rate and thermal structure determined from progressive magnetization of the dacite dome at Mount St. Helens, Washington. *Bulletin of the Seismological Society of America*, **95**: 2763–2780.
- Ishido, T., 2004. Electrokinetic mechanism for the “W”-shaped self-potential profile on volcanoes. *Geophysical Research Letters*, **31**: L22601 (doi: 10.1029/2004GL020964).
- Johnston, M.J.S., 1997. Review of electrical and magnetic fields accompanying seismic and volcanic activity. *Surveys in Geophysics*, **18**: 441–475.
- Johnston, M.J.S., Mueller, R.J., and Dvorak, J., 1981. Volcano-magnetic observations during eruptions May–August 1980. *US Geological Survey Professional Papers*, **1250**: 183–189.

Mueller, R.J., and Johnston, M.J.S., 1989. Large-scale magnetic field perturbations arising from the 18 May 1980, eruption from Mount St. Helens, Washington. *Physics of the Earth and Planetary Interiors*, **57**: 23–31.

Sasai, Y., Zlotnicki, J., Nishida, Y., Yvetot, P., Morat, P., Murakami, H., Tanaka, Y., Ishikawa, Y., Koyama, S., and Sekiguchi, W., 1997. Electromagnetic monitoring of Miyake-Jima volcano, Izu-Bonin Arc, Japan: a preliminary report. *Journal of Geomagnetism and Geoelectricity*, **49**: 1293–1316.

Yukutake, T., Yoshino, T., Utada, H., Watanabe, H., Hamano, Y., and Shimomura, T., 1990. Changes in the electrical resistivity of the central cone, Mihara-yama, of Oshima volcano observed by a direct current method. *Journal of Geomagnetism and Geoelectricity*, **42**: 151–168.

Zlotnicki, J., 1995. Geomagnetic surveying methods. In McGuire, W., Kilburn, C., and Murray, J. (eds.), *Monitoring Active Volcanoes*. London: University College London Press, pp. 275–296.

Zlotnicki, J., Sasai, Y., Nishida, Y., Uyeshima, M., Takahashi, Y., and Donnadieu, G., 2003. Resistivity and self-potential changes associated with volcanic activity: the 8 July 2000 Miyake-Jima eruption (Japan). *Earth and Planetary Science Letters*, **205**: 139–154.

Cross-references

Depth to Curie Temperature
 Electromagnetic Induction (EM)
 Geomagnetic Spectrum, temporal
 Gravity-Inertio Waves and Inertial Oscillations
 Ionosphere
 Magnetotellurics
 Seismo-Electromagnetic Effects

Au1

Author Query Form

Encyclopedia of Geomagnetism and Paleomagnetism
Alpha - V

Query Refs.	Details Required	Author's response
AU1	Please note that no article with the title "Electromagnetic Induction (EM)" exists in this Encyclopedia.	